Fluorescent intercalator displacement replacement (FIDR) assay: determination of relative thermodynamic and kinetic parameters in triplex formation—a case study using triplex-forming LNAs

Sujay P. Sau[1], Pawan Kumar[1,2], Pawan K. Sharma[2] and Patrick J. Hrdlicka[1,*]

[1]Department of Chemistry, University of Idaho, PO Box 442343, Moscow, ID 83844-2343, USA and
[2]Department of Chemistry, Kurukshetra University, Kurukshetra 136119, India

ABSTRACT

Triplex forming oligonucleotides (TFOs) are the most commonly used approach for site-specific targeting of double stranded DNA (dsDNA). Important parameters describing triplex formation include equilibrium binding constants (K_{eq}) and association/dissociation rate constants (k_{on} and k_{off}). The 'fluorescent intercalator displacement replacement' (FIDR) assay is introduced herein as an operationally simple approach toward determination of these parameters for triplexes involving TC-motif TFOs. Briefly described, relative rate constants are determined from fluorescence intensity changes upon: (i) TFO-mediated displacement of pre-intercalated and fluorescent ethidium from dsDNA targets (triplex association) and (ii) Watson–Crick complement-mediated displacement of the TFO and replacement with ethidium (triplex dissociation). The assay is used to characterize triplexes between purine-rich dsDNA targets and TC-motif TFOs modified with six different locked nucleic acid (LNA) monomers, i.e. conventional and C5-alkynyl-functionalized LNA and α-L-LNA pyrimidine monomers. All of the studied monomers increase triplex stability by decreasing the triplex dissociation rate. LNA-modified TFOs form more stable triplexes than α-L-LNA-modified counterparts owing to slower triplex dissociation. Triplexes modified with C5-(3-aminopropyn-1-yl)-LNA-U monomer Z are particularly stable. The study demonstrates that three affinity-enhancing features can be combined into one high-affinity TFO monomer: conformational restriction of the sugar ring, expansion of the pyrimidine π-stacking surface and introduction of an exocyclic amine.

INTRODUCTION

Development of agents that site-specifically target double stranded DNA (dsDNA) has attracted considerable attention in the past decades, due to the prospect of access to enabling research tools and new types of therapeutic and diagnostic probes (1,2). Despite significant progress with polyamides (3), peptide nucleic acids (4–7) and other probe technologies (8,9), the use of chemically modified triplex forming oligonucleotides (TFOs) remains the most widely studied approach toward this end (10). TFOs bind in the major groove of dsDNA, where they form hydrogen bonds to a purine-rich target strand. The relative orientation of the TFO depends on its composition; for example, TFOs that are solely composed of pyrimidines (TC-motif TFOs), bind with parallel orientation relative to the purine-rich strand.

To be active in biological settings, TFOs should preferentially: (i) result in the formation of thermodynamically stable triplexes, (ii) associate quickly with their dsDNA target, while (iii) displaying slow dissociation (11). The parameters used to describe these characteristics include the equilibrium constant for triplex formation (K_{eq}), and the rate constants for association and dissociation, k_{on} and k_{off}. Determination of triplex-to-duplex denaturation temperatures (T_m's) via temperature-controlled absorbance measurements is a popular and straightforward approach toward estimating the thermostability of triplexes (12). However, significant hysteresis is often observed, due to the slow kinetics of triplex formation, which skews the determined T_m values.
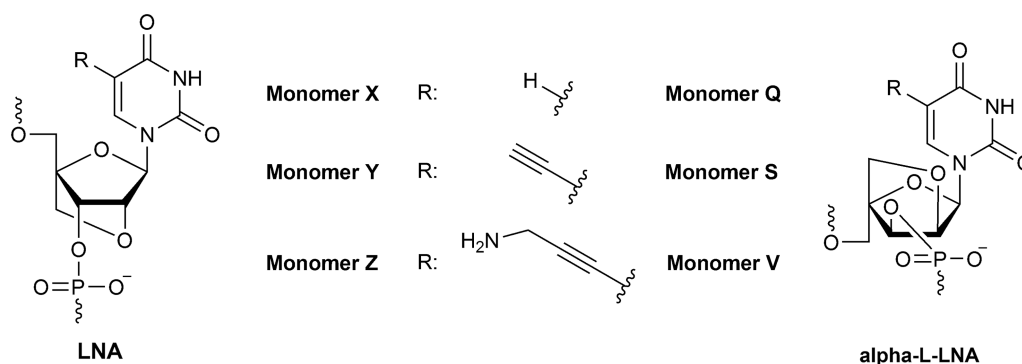
Figure 1. LNA and α-L-LNA monomers studied herein.

Several techniques and assays have been developed to study the kinetics of triplex formation including non-equilibrium thermal denaturation hysteresis analysis (13,14), kinetic footprinting assays (13,15,16), biomolecular interaction analysis via surface plasmon resonance (17,18), UV absorbance decay analysis (19) and FRET-based assays (13,20). While powerful, most of these approaches are technically challenging, resource-intensive and require probe labeling or specialized instrumentation. Development of an operationally simple assay that allows for determination of relative thermodynamic and kinetic parameters involved in triplex formation would therefore be desirable and facilitate comparative screening of established and new TFO-chemistries.

Fluorescent intercalator displacement assays have been used to study interactions and determine binding affinities of small ligands (21–24) as well as TC-motif TFOs (25) to dsDNA targets. In the first part of this article, we describe the concept of, and underlying theoretical model for, the operationally simple 'fluorescent intercalator displacement replacement' (FIDR) assay, which provides access to relative rate and equilibrium binding constants involved in triplex formation. In the second part, we use the FIDR assay to characterize triplexes between dsDNA targets and TC-motif TFOs, which are modified with six different locked nucleic acid (LNA) (26) monomers (Figure 1).

TC-motif TFOs modified with conventional LNA-T (27,28) and α-L-LNA-T (29) monomers **X** and **Q** (Figure 1) substantially increase the thermostability of triplexes relative to reference TFOs (18,30–34). Kinetics experiments show this to be the result of significantly slower triplex dissociation (18,33,34). The structural mechanisms accounting for these trends are not fully understood but seem to involve TFO preorganization (favorable entropy) and formation of bifurcated hydrogen bonds between the TFO and Watson–Crick duplex (slower dissociation) (31,32).

The interesting properties of LNA-modified TC-motif TFOs has spurred development of LNA analogues that display even more favorable triplex hybridization characteristics (35–40). The majority of these studies have focused on monomers in which the dioxabicyclo-[2.2.1]-heptane skeleton of LNA is modified. Following a different approach, we recently set out to explore monomers

that combine structural features of LNA and C5-alkynyl-functionalized DNA monomers; the latter are known to moderately increase triplex thermostability by enhancing base stacking interactions (41–44). Initial motivation for this approach came from studies on TFOs modified with C5-alkynyl-functionalized RNA monomers, which display greater affinity toward dsDNA targets than reference TFOs modified with the corresponding non-functionalized RNA monomers or C5-alkynyl-functionalized DNA monomers (13,45–47). Our preliminary results have, indeed, demonstrated that TC-motif TFOs modified with C5-alkynyl-functionalized LNA monomers **Y** and **Z** (48) (Figure 1) display higher thermal affinity toward purine-rich dsDNA targets than conventional LNA TFOs (ΔT_m/mod values between +1.1°C and +2.8°C higher than for LNA TFOs) (49).

We utilize the FIDR assay to study the hybridization characteristics of triplexes composed of TC-motif TFOs modified with monomers **Q–Z** (Figure 1), in order to explore if combination of structural elements from C5-alkynyl-functionalized DNA monomers and conformationally restricted nucleotides is a general approach toward high-affinity TFO monomers.

MATERIALS AND METHODS

Synthesis of ONs

TFOs modified with LNA monomers **X–Z** (Figure 1) were prepared and characterized with respect to identity (MALDI-MS) and purity (>80%, ion-pair reverse-phase HPLC) in our preliminary study (49). Novel TFOs modified with α-L-LNA monomers **Q/S/V** (Figure 1) were prepared by incorporating the appropriately protected phosphoramidites into ONs via machine-assisted solid-phase DNA synthesis (0.2 μmol scale) using 4,5-dicyanoimidazole as the activator and extended hand-coupling (15 min) and oxidation (45 s). This resulted in stepwise coupling yields of ~98%, ~97% and ~90%, respectively. The corresponding phosphoramidite of monomer **Q** was obtained from commercial sources; the synthesis of the corresponding phosphoramidites of monomers **S** and **V** will be reported elsewhere (the 3-aminopropyn-1-yl group was protected with as a trifluoroacetamide during ON synthesis). Cleavage from

solid support (succinyl linked LCAA-CPG, pore size: 500 Å), removal of protecting groups and conversion of O4-triazolyl-dT monomers into 5-methyl-dC monomers (mC), was accomplished upon treatment with 32% aq. ammonia (24–48 h, rt). All ONs were purified by RP-HPLC in the DMT-on mode on a Varian Prostar HPLC system equipped with an XTerra MS C18 column using the following representative gradient (flow rate 1.2 ml/min): 100 vol% buffer A for 2 min, $100 \rightarrow 30$ vol% buffer A in buffer B over 48 min, $30 \rightarrow 0$ vol% buffer A in buffer B over 14 min and 100 vol% buffer B for 5 min, where buffer A is 0.05 M TEAA (triethyl ammonium acetate) pH 7.4 and buffer B is 75% MeCN in H_2O v/v. The DMTr-group was cleaved using 80% aq. AcOH, followed by precipitation of the crude ONs (acetone, $-18°C$, 12–16 h). The identity of synthesized ONs was established through analysis on a quadrupole time-of-flight tandem mass spectrometer equipped with a MALDI source (positive ion mode) using anthranilic acid as a matrix (Supplementary Table S1), while purity ($>80\%$) was verified by ion-pair reverse phase HPLC running in analytical mode.

Experimental protocol of the FIDR assay

A 1.4-ml semi-micro fluorescence quartz cell was loaded with 1.0 ml of a 1.0 μM solution of pre-annealed target duplex in TNM buffer (pH 7.2, 50 mM Tris–Cl containing 150 mM NaCl and 5 mM $MgCl_2$) and 20 μl of 0.50 mM EtBr (final concentration ~10 μM). After equilibrating at 20°C for 10 min, an aqueous solution of TFO (<10 μl, final concentration ~1.0 μM) was added to this solution. The fluorescence emission decay was recorded until steady-state was reached ($\lambda_{ex} = 530$ nm; $\lambda_{em} = 600$ nm). An excess of single-stranded DNA complementary to the TFO (cTFO) was then added (33 μl, ~4.0 μM final concentration) and the increase in fluorescence intensity monitored until steady-state was reached. The fluorescence emission profile representing triplex association was fitted to Equation (4), which is used to determine the relative association rate constant for triplex formation;

the fluorescence emission profile representing triplex dissociation was fitted to Equation (8), which was used to determine the relative rate constant for triplex dissociation (see 'Results and Discussion' section).

Thermal denaturation studies

A 1.0-ml solution containing 1.0 nmol of each strand (buffer: 140 mM KCl and 0.1 mM EDTA, pH 7.0 adjusted with 10 mM NaH_2PO_4 and 5 mM Na_2HPO_4) in quartz optical cells with path-lengths of 1.0 cm, was heated (~80°C, 5 min), cooled to room temperature and incubated overnight. Thermal denaturation profiles were recorded on a Cary 100 UV/VIS spectrophotometer equipped with a 12-cell Peltier temperature controller using a ramp of 0.5°C/min. Thermal denaturation temperatures for triplex-to-duplex transitions were determined as the first derivative of difference thermal denaturation profiles (dA_{260} versus T) (32), which were obtained by subtracting the thermal denaturation profile of the dsDNA target (included as one of the samples in the multicell holder of the spectrophotometer) from the raw thermal denaturation profile of triplex solution. Reported T_m values are an average of at least two experiments within $\pm 1.0°C$.

RESULTS AND DISCUSSION

Assay overview

The concept of the FIDR assay is shown in Figure 2. The assay relies on the fact that ethidium generally: (i) displays greater fluorescence intensity upon intercalation into dsDNA than in free solution and (ii) has higher affinity toward dsDNA than triplexes involving TC-motif TFOs, while being readily displaced by groove binding agents such as TFOs (50).

Addition of a TC-motif TFO to a pre-equilibrated solution of a dsDNA target and excess EtBr, results in triplex formation and partial displacement of intercalated ethidium (Figure 2, $A \rightarrow B$). The progress of triplex
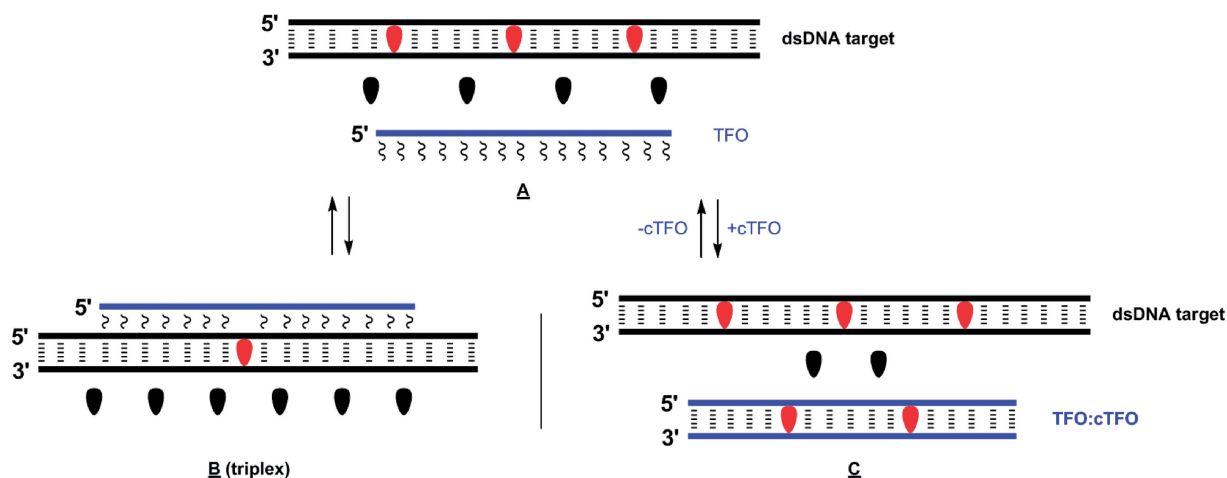
Figure 2. Illustration of the fluorescent intercalator displacement replacement (FIDR) assay. Droplet denotes ethidium bromide. Straight and squiggly bonds denote Watson–Crick and Hoogsteen bonds, respectively.
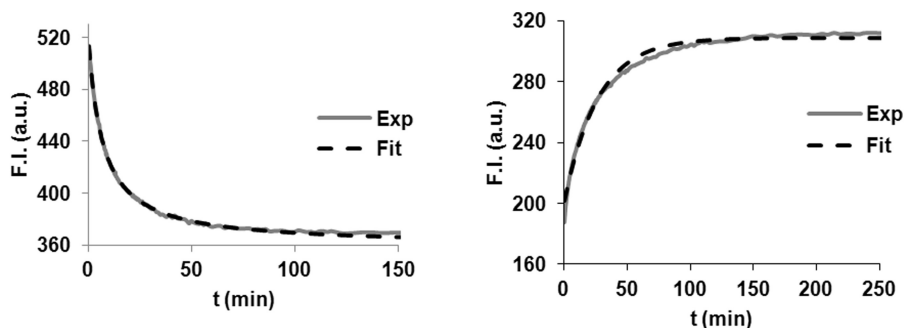
Figure 3. Fluorescence emission profiles ($\lambda_{ex} = 530\,nm$; $\lambda_{em} = 600\,nm$) during association (left) and dissociation (right) of the triplex between representative LNA-TFO **X1** and dsDNA target (see Table 2 for sequences). Experimental conditions: [TFO] = 1.0 µM, [dsDNA target] = 1.0 µM, [EtBr] = 10 µM, [cTFO] = 4.0 µM in TNM buffer (pH 7.2, 50 mM Tris–Cl, 150 mM NaCl and 5 mM MgCl$_2$) at $T = 20°C$. Experimental profiles are fitted to Equations (4) and (8) (see below), respectively.

formation can be monitored by the decrease in fluorescence emission that results due to ethidium displacement (Figure 3—left). Once a plateau is reached, the TFO is displaced from the triplex by adding its single stranded Watson–Crick complement (cTFO) (Figure 2, B → C via A). This process, i.e. triplex dissociation and formation of two DNA duplexes, results in increased intercalation of ethidium and fluorescence emission (Figure 3—right). Relative triplex association and dissociation rate constants are obtained by fitting fluorescence emission traces to expressions for second and first order reaction rate equations, respectively (see next section).

Theoretical model for FIDR assay

Triplex formation between the TC-motif TFO and dsDNA target is approximated by the following model, which is not adjusted for contributions from EtBr:

$$\text{dsDNA} + \text{TFO} \underset{k_{off}}{\overset{k_{on}}{\rightleftharpoons}} \text{triplex} \qquad (1)$$

At the chosen conditions, i.e. at experimental temperatures significantly below the triplex-to-duplex transition temperature, triplex association is more rapid and prominent than triplex dissociation. Furthermore, the weak and rapidly equilibrating intercalative binding of ethidium bromide is assumed not to interfere with triplex formation. Triplex formation is accordingly treated as a unidirectional, bimolecular and rate-limiting reaction that follows second order reaction kinetics:

$$-\frac{d[\text{dsDNA}]}{dt} = \frac{d[\text{triplex}]}{dt} = k_{on} \cdot [\text{dsDNA}] \cdot [\text{TFO}] \qquad (2)$$

where k_{on} is the apparent rate constant for triplex association. Solving Equation (2) (for additional details, see Supplementary Data) gives:

$$\frac{1}{[dsDNA]} - \frac{1}{[dsDNA]_0} = k_{on} \cdot t \qquad (3)$$

where $[\text{dsDNA}]_0$ is the initial dsDNA concentration. According to the FIDR concept (Figure 2, A → B), $[\text{dsDNA}]_0$ is proportional to $(F_{initial} - F_{final})$ while $[\text{dsDNA}]$ is proportional to $(F_t - F_{final})$, where $F_{initial}$, F_t

and F_{final} denote fluorescence intensity of EtBr before TFO addition, at a time after TFO addition and at steady-state, respectively. Insertion into Equation (3) yields the following fitting equation:

$$\frac{(F_{initial} - F_t)}{(F_t - F_{final}) \cdot [dsDNA]_0} = k_{on} \cdot t \qquad (4)$$

Equation (5), which also does not take contributions from EtBr into account, describes triplex dissociation in the presence of excess single-stranded Watson–Crick complement to the TFO (cTFO). The role of cTFO is to sequester free TFO and promote triplex dissociation at experimental temperatures that otherwise favor the triplex form.

$$\text{triplex} \underset{k_{on}}{\overset{k_{off}}{\rightleftharpoons}} \text{dsDNA} + \text{TFO} \underset{+\text{cTFO}}{\overset{k_2}{\rightarrow}} \text{dsDNA} + \text{cTFO} : \text{TFO}$$

$$(5)$$
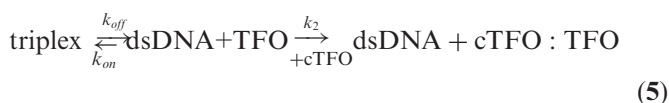
Assuming that triplex dissociation is significantly slower than triplex association and cTFO:TFO duplex formation ($k_{off} \sim 10^{-5}\,s^{-1}$; $k_{on} \sim 10^3\,M^{-1}s^{-1}$; $k_2 \sim 10^7\,M^{-1}s^{-1}$) (51) and that the equilibrating intercalative binding of ethidium bromide is weak and rapid, the rate-limiting triplex dissociation is approximated as an unidirectional reaction with first order reaction kinetics:

$$-\frac{d[\text{triplex}]}{dt} = k_{off} \cdot [\text{triplex}] \qquad (6)$$

where k_{off} is the apparent rate constant for triplex dissociation. Solving Equation (6) gives:

$$[triplex] = [triplex]_0 \cdot e^{-k_{off} \cdot t} \qquad (7)$$

where $[\text{triplex}]_0$ is the initial triplex concentration. It follows from the FIDR concept (Figure 2, B → C) that $[\text{triplex}]_0$ is proportional to $(F_{initial} - F_{final})$, while $[\text{triplex}]$ is proportional to $(F_t - F_{final})$, where $F_{initial}$, F_t and F_{final} denote fluorescence intensity of EtBr before cTFO addition, at a time after cTFO addition and at steady-state, respectively. Insertion into Equation (7) gives the following fitting equation:

$$(F_t - F_{final}) = (F_{initial} - F_{final}) \cdot e^{-k_{off} \cdot t} \qquad (8)$$

Table 1. Optimization of the FIDR assay using the triplex between representative LNA-TFO **X1** and dsDNA target at various EtBr and Mg^{2+} concentrations; optimized conditions shown in bold[a]

Entry	EtBr (μM)	Mg^{2+} (mM)	k_{on} ($\times 10^3$)[b] ($M^{-1}s^{-1}$)	k_{off} ($\times 10^{-5}$)[c] (s^{-1})	K_{eq} ($\times 10^7$)[d] (M^{-1})	$T_{0.5on}$[e] (min)	$T_{0.5off}$[f] (min)
1	5	5	1.28 ± 0.1	24.3 ± 2.0	0.53 ± 0.0	13.1	47.7
2	**10**	**5**	$\mathbf{2.38 \pm 0.0}$	$\mathbf{48.5 \pm 4.0}$	$\mathbf{0.50 \pm 0.0}$	**7.0**	**23.9**
3	20	5	4.89 ± 0.1	259 ± 3.9	0.19 ± 0.0	3.4	4.5
4	10	10	4.22 ± 0.2	89.3 ± 3.1	0.47 ± 0.0	4.0	12.9
5	10	20	7.0 ± 0.5	105 ± 4.1	0.67 ± 0.0	2.4	11.1

[a]For sequences of **X1** and dsDNA target, see Table 2. Experimental conditions: [TFO] = 1.0 μM, [dsDNA target] = 1.0 μM, [cTFO] = 4.0 μM in TNM buffer (pH 7.2, 50 mM Tris–Cl, 150 mM NaCl and 5 mM $MgCl_2$) at T = 20°C.
[b]Obtained by fitting data to Equation (4).
[c]Obtained by fitting data to Equation (8).
[d]$K_{eq} = k_{on}/k_{off}$.
[e]$T_{0.5\ on} = 1/C_0 k_{on}$, where C_0 is [TFO]$_{initial}$.
[f]$T_{0.5\ off} = \ln 2/k_{off}$.

The strong correlation between the experimental and fitted profiles suggests that the underlying approximations (e.g. significantly faster triplex association than triplex dissociation) are met for the TFOs studied herein (*vide infra*).

Optimization of FIDR assay

The influence of EtBr on the FIDR assay was studied first (Table 1). Toward this end, the triplex between the representative TC-motif LNA-TFO **X1** and its complementary dsDNA target was studied in a TNM buffer (pH 7.2, 50 mM Tris–Cl, 150 mM NaCl and 5 mM $MgCl_2$) at T = 20°C using [TFO] = 1.0 μM, [dsDNA target] = 1.0 μM and [cTFO] = 4.0 μM. $MgCl_2$ was included to accelerate and stabilize triplex formation (52). Increased EtBr levels result in faster association and dissociation of the triplex (Table 1) and decreased triplex thermostability (data not shown), which is in agreement with previous reports (50). Interestingly, the relative equilibrium constant for triplex formation, K_{eq}, is very similar when using 5 or 10 μM EtBr, but lower with 20 μM EtBr. We note that one of the underlying assumptions for the FIDR assay, i.e. triplex dissociation being significantly slower than triplex association [see Equations (5) and (6)], no longer is met at [EtBr] = 20 μM (compare $T_{0.5,on}$ and $T_{0.5,off}$ entries 1–3, Table 1). Subsequent experiments utilized 10 μM EtBr as a suitable compromise between fast triplex formation and sufficient triplex thermostability. Titration experiments revealed that only ~40% of the added EtBr intercalates into the dsDNA target prior to TFO-addition (~0.2 equivalents EtBr per base pair, results not shown).

Increased concentrations of $MgCl_2$ also result in faster association and dissociation (entries 2, 4 and 5, Table 1). K_{eq}-values are virtually identical when using 5 or 10 mM $MgCl_2$, but noticeably higher at 20 mM $MgCl_2$. The underlying structural basis for this phenomenon is not fully understood, but may be linked to the well-known property of high Mg^{2+} concentrations in promoting formation of higher order structures. Subsequent FIDR experiments used 5 mM $MgCl_2$ (entry 2, Table 1).

Application of the FIDR assay using LNA-modified reference triplexes

We evaluated the FIDR assay against reference triplexes composed of dsDNA targets and TC-motif TFOs modified with conventional LNA-T and α-L-LNA-T monomers **X** and **Q** (Figure 1). Monomers were incorporated once, three and six times into a 15-mer TFO that has previously been used to evaluate LNA, ENA and other bridged nucleic acid (BNA) monomers (Table 2) (36). 5-Methyl-2′-deoxycytidine monomers, rather than 2′-deoxycytidine monomers, were used to increase the affinity of the TFOs toward dsDNA at neutral pH (53).

In agreement with previous studies, the stability of triplexes increases progressively with higher LNA content (K_{eq}: **X1** < **X2** ≤ **X3** < **X4**, Table 2). This trend correlates strongly with the rate constants for triplex dissociation, which decrease sharply with higher LNA content (see k_{off} for **X**-series, Table 2). As a result, the triplex dissociation half-lives increase from ~24 min for **X1** to 270 min for **X4** (Table 2). TFOs with three or fewer incorporations of LNA monomer **X** display similar apparent rate constants for triplex association, while k_{on} for the densely modified **X4** is 2-fold higher (Table 2). The remarkable stability of the triplex involving **X4** ($K_d \sim 10$ nM) is, accordingly, the result of faster association and slower dissociation. As expected (see 'Theoretical Model for FIDR Assay' section), triplex association is considerably faster than triplex dissociation, especially for more highly modified triplexes ($T_{0.5\ on} << T_{0.5\ off}$, Table 2).

α-L-LNA TFOs display similar triplex association rates as their LNA counterparts and also result in slower triplex dissociation with increasing levels of modification (see **Q**-series, Table 2). However, triplex dissociation occurs 2- to 4-fold faster than in LNA-modified triplexes, which is the main reason for the lower stability of triplexes involving α-L-LNA TFOs (compare k_{off} and K_d for **Q**- versus **X**-series, Table 2).

In spite of the numerous approximations, the results from the FIDR assay—i.e. trends and relative values of K_{eq}, k_{on} and k_{off}—are in good agreement with previous reports,

Table 2. Triplex binding kinetics for LNA- and α-L-LNA-modified TC-motif TFOs[a]

ON	Sequence (5′ → 3′)	k_{on} ($\times 10^3$) ($M^{-1}s^{-1}$)	k_{off} ($\times 10^{-5}$) (s^{-1})	$t_{1/2,on}$ (min)	$t_{1/2,off}$ (min)	K_{eq} ($\times 10^7$) (M^{-1})	K_d (nM)	T_m [$\Delta T_m/mod$] (°C)
X1	TTTTTCT**X**TCTCTCT	2.39 ± 0.1	48.5 ± 4.0	7.0	23.9	0.50 ± 0.0	202 ± 15	40.0 [+11.0]
X2	TTTT**X**CTT**X**CTC**X**CT	1.80 ± 0.2	5.93 ± 0.4	9.3	196	3.10 ± 0.6	33 ± 7	48.5 [+6.5]
X3	TTTT**X**CT**X**TC**X**CTCT	2.09 ± 0.1	5.68 ± 0.5	8.0	204	3.71 ± 0.5	27 ± 4	53.5 [+8.2]
X4	TT**X**T**X**C**X**T**X**C**X**C**X**CT	4.42 ± 0.4	4.29 ± 0.4	3.8	270	10.4 ± 1.8	10 ± 3	61.0 [+5.3]
Y1	TTTTTCT**Y**TCTCTCT	2.38 ± 0.0	26.3 ± 0.2	7.0	43.9	0.91 ± 0.0	111 ± 2	42.5 [+13.5]
Y2	TTTT**Y**CTT**Y**CTC**Y**CT	1.87 ± 0.4	5.55 ± 0.9	9.1	212	3.53 ± 0.0	29 ± 0.1	54.0 [+8.3]
Y3	TTTT**Y**CT**Y**TC**Y**CTCT	3.03 ± 0.5	5.62 ± 1.2	5.6	211	5.43 ± 0.3	19 ± 1	59.5 [+10.2]
Y4	TT**Y**T**Y**C**Y**T**Y**C**Y**C**Y**CT	4.23 ± 0.0	8.68 ± 0.2	3.9	133	4.88 ± 0.2	21 ± 1	67.5 [+6.4]
Z2	TTTT**Z**CTT**Z**CTC**Z**CT	2.17 ± 0.3	5.33 ± 0.4	7.8	218	4.16 ± 0.2	24 ± 1	57.0 [+9.3]
Z3	TTTT**Z**CT**Z**TC**Z**CTCT	3.92 ± 0.6	5.56 ± 0.3	4.3	208	7.09 ± 1.5	14 ± 6	60.0 [+10.3]
Q1	TTTTTCT**Q**TCTCTCT	2.69 ± 0.4	113 ± 2.3	6.3	10.2	0.24 ± 0.0	422 ± 78	35.5 [+6.5]
Q2	TTTT**Q**CTT**Q**CTC**Q**CT	2.17 ± 0.1	12.7 ± 2.1	7.7	92.5	1.74 ± 0.3	58 ± 13	43.5 [+4.8]
Q3	TTTT**Q**CT**Q**TC**Q**CTCT	2.08 ± 0.1	17.2 ± 1.5	8.0	67.4	1.22 ± 0.2	82 ± 18	44.5 [+5.2]
Q4	TT**Q**T**Q**C**Q**T**Q**C**Q**C**Q**CT	3.41 ± 0.3	17.1 ± 0.9	4.9	67.6	1.99 ± 0.2	50 ± 6	37.5 [+1.4]
S1	TTTTTCT**S**TCTCTCT	2.42 ± 0.3	77.8 ± 9.6	7.0	15.0	0.31 ± 0.0	321 ± 18	37.5 [+8.5]
S2	TTTT**S**CTT**S**CTC**S**CT	2.77 ± 0.2	7.15 ± 0.4	6.0	162	3.89 ± 0.5	26 ± 3	48.0 [+6.3]
S3	TTTT**S**CT**S**TC**S**CTCT	2.80 ± 0.3	9.27 ± 1.0	6.0	126	3.06 ± 0.5	33 ± 5	50.0 [+7.0]
S4	TT**S**T**S**C**S**T**S**C**S**C**S**CT	4.88 ± 0.8	6.83 ± 0.3	3.5	169	7.17 ± 1.4	14 ± 2	45.5 [+2.8]
V1	TTTTTCT**V**TCTCTCT	2.87 ± 0.4	78.3 ± 3.9	5.9	14.8	0.37 ± 0.1	274 ± 38	37.0 [+8.0]
V2	TTTT**V**CTT**V**CTC**V**CT	2.31 ± 0.2	12.1 ± 0.9	7.3	95.6	1.92 ± 0.3	53 ± 10	46.0 [+5.7]
V3	TTTT**V**CT**V**TC**V**CTCT	2.69 ± 0.4	33.8 ± 3.1	6.3	34.4	0.81 ± 0.2	124 ± 38	45.5 [+5.5]

[a]Structures of monomers shown in Figure 1. 'C' denotes 5-methyl-2′-deoxycytidine monomers. dsDNA target sequence (TFO binding region underlined): 5′-GCT <u>AAA AAG AAA GAG AGA</u> TCG-3′, 3′-CGA <u>TTT TTC TTT CTC TCT</u> ACG-5′. **Z1**, **Z4** and **V4** were not studied. '±' denotes SD; ND, not determined. Experimental conditions for parameter determination via FIDR assay (all except last column) are as described in Figure 3. Last column: T_m's determined as first derivative of differential thermal denaturation curves (A_{260} versus T) (32) recorded in a pH 7.0 phosphate buffer solution (pH adjusted with 10 mM NaH$_2$PO$_4$/5 mM Na$_2$HPO$_4$) containing 140 mM KCl and 10 mM EDTA, and using 1.0 μM of each strand and 0.5°C/min temperature gradient. T_m's are averages of at least two independent measurements within 1°C and given relative to unmodified reference DNA TFO 5′-TTT TTC TTT CTC TCT: T_m = 29.0°C. The T_m of the reference triplex was too low to reliably obtain parameters via the FIDR assay.

which have demonstrated that the increased stability of triplexes involving LNA- and α-L-LNA-modified TC-motif TFOs is linked to slower dissociation kinetics (18,33,34). The present study represents the first direct comparison between these two classes of TFO-monomers and identifies important differences in dissociation kinetics. NMR solution structures of intramolecular dsDNA:LNA triplexes feature bifurcated hydrogen bonds between the TFO and Watson–Crick duplex, which have led to the hypothesis that the slow dissociation kinetics are related to slow opening of these hydrogen bond networks (31). In absence of NMR structures, we speculate that such networks are less prevalent in dsDNA:α-L-LNA triplexes, leading to faster dissociation and lower triplex stability relative to LNA modified triplexes.

Characterization of triplexes modified with C5-functionalized LNA/α-L-LNA monomers

After validating the FIDR assay against reference triplexes, we applied the assay in the characterization of triplexes modified with C5-functionalized LNA-U or α-L-LNA-U monomers **S/V/Y/Z** (Figure 1).

Triplexes between dsDNA targets and TC-motif TFOs with one or three incorporations of C5-ethynyl LNA-U monomer **Y** are more stable than the corresponding LNA-modified triplexes, while the extensively modified **Y4**:dsDNA is less stable (compare K_{eq} for **Y**- and **X**-series, Table 2). The latter observation is surprising considering

that: (i) the thermostability of **Y4**:dsDNA is very high (divergence between K_{eq} and T_m will be discussed later) and (ii) triplexes that are densely modified with C5-propynyl 2′-deoxyuridine monomers are highly thermostable (42,45). We speculate that the combination of a conformationally restricted LNA skeleton and an ethynyl side chain is favorable at low modification densities due to enhanced base-stacking, whereas it imposes partially unfavorable steric interactions in densely modified triplexes. The correlation between triplex stability and kinetics in the **Y**-series is not obvious. For example, the greater stability of **Y1**:dsDNA relative to **X1**:dsDNA is linked to markedly slower dissociation, whereas the greater stability of **Y3**:dsDNA is correlated with faster association. In contrast, the extensively modified **Y4**:dsDNA displays much faster dissociation kinetics that its LNA-modified counterpart, perhaps due to aforementioned unfavorable steric interactions (compare k_{on} and k_{off} for **Y**- and **X**-series, Table 2).

TC-motif TFOs with three incorporations of C5-(3-aminopropyn-1-yl)-LNA-U monomer **Z** display slightly larger relative association rate constants than the corresponding **X**- or **Y**-series TFOs but similar dissociation rate constants (Table 2). We propose that partially positively charged 'patches' of C5-(3-aminopropyn-1-yl)-groups enable cooperative clamping of the negatively charged dsDNA target, in an analogous manner as suggested for TFOs modified with the corresponding DNA
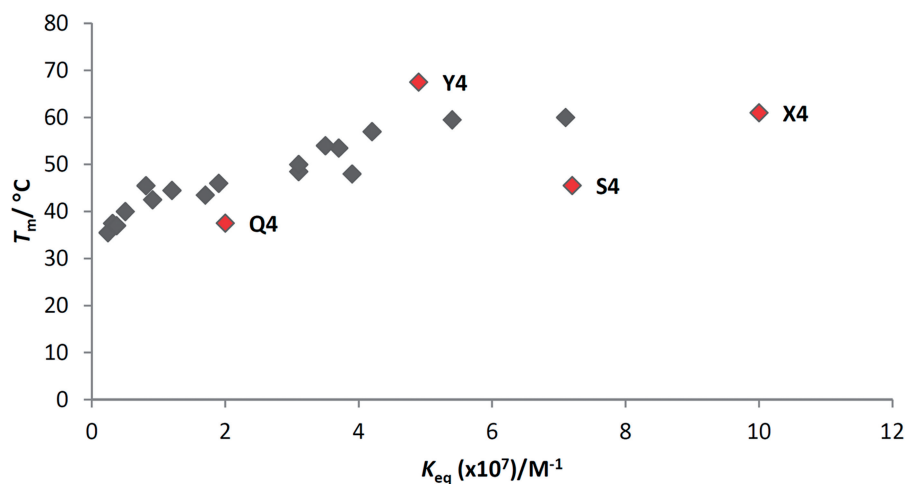
Figure 4. Scatter plot of triplex T_m's determined from thermal denaturation curves as a function of triplex K_{eq} values determined by the FIDR assay. Data points for triplexes involving **B4**-series TFOs are highlighted.

monomer (45). The observed trend in triplex stability, i.e. monomer $X \leq Y < Z$, suggests that it is possible to combine three affinity-enhancing features into one high-affinity TFO monomer: conformational restriction of the sugar ring (LNA skeleton), increased stacking interactions (alkynyl substituent) and electrostatic interactions of ammonium group with negatively charged strands.

The association of triplexes involving TC-motif TFOs that are densely modified with C5-ethynyl-α-L-LNA-U monomer **S** occurs more rapidly than with conventional α-L-LNA TFOs (compare k_{on} for **S2**–**S4** with **Q2**–**Q4**, Table 2). This, coupled with considerably slower triplex dissociation, results in extensive stabilization of **S**-modified triplexes relative to α-L-LNA modified triplexes (compare k_{off} and K_{eq} of **S**- versus **Q**-series, Table 2). In fact, introduction of a C5-ethynyl group has a far greater triplex stabilizing effect in the α-L-LNA than LNA series, rendering **S**-modified triplexes of similar stability as triplexes composed of conventional LNA TFOs (compare K_{eq} of **S**- versus **Q**- and **Y**- versus **X**-series, Table 2).

Triplexes between dsDNA and TC-motif TFOs modified with three C5-(3-aminopropyn-1-yl)-α-L-LNA-U monomer **V** are less stable than corresponding **S**-modified triplexes (K_{eq}: $Q \leq V < S$, Table 2), which contrasts the influence of substituents in the LNA-series. Their lower stability is linked with markedly faster dissociation kinetics, while the similar association kinetics suggest that C5-(3-aminopropyn-1-yl)-groups do not play important roles in clamping dsDNA targets in this series.

Correlation between K_{eq} and T_m

The thermal denaturation temperatures of the triplex-to-duplex transitions were determined under typical experimental conditions (Table 2) and plotted as a function of their corresponding K_{eq} values (Figure 4). Visual inspection reveals that the data points for triplexes involving the highly modified **B4**-series TFOs are located outside from

the main cluster of data points. This likely reflects that thermal denaturation curves for the more highly modified triplexes are not recorded under equilibrium conditions (12). Indeed, we note that triplexes modified with **B4**-series TFOs generally display faster association and slower dissociation kinetics than the other TFO series (Table 2). We argue that K_{eq}-values determined via the FIDR assay, as opposed to T_m values from thermal denaturation experiments, are a more reliable—yet convenient—approach for estimation of triplex thermostability.

CONCLUSION

The FIDR assay presented herein provides operationally simple access to thermodynamic and kinetic parameters associated with nucleic acid triplexes, i.e. relative rate constants for association/dissociation and equilibrium binding constants. While we have only used the assay to compare hybridization characteristics of LNA- and α-L-LNA-modified TC-motif TFOs, we expect the assay to be broadly applicable for characterization of triplexes involving other TC-motif TFOs, provided that the underlying assumptions are met (e.g. ethidium displaying greater affinity toward dsDNA than triplexes). It is important to note that this will not always be the case. For example, ethidium has low affinity toward duplexes with long adenines stretches and the FIDR assay will, most likely, not be applicable for characterization of triplexes composed of (T):(dA):(T) stretches (54). Future studies will delineate the full scope of the FIDR assay and its value as a screening tool for identification of promising TFO-chemistries.

All of the LNA analogues studied herein increase triplex stability by decreasing the rate of triplex dissociation (K_{eq} trend: $Z > Y > X \geq S > V \sim Q$). The data demonstrate that it is possible to combine three structural features to give high-affinity TFO monomers, i.e. conformational restriction of the sugar ring (LNA skeleton), increased π-stacking surface of the nucleobase (alkynyl substituent)

and electrostatic screening of negatively charged strands (ammonium group). TC-motif TFOs modified with C5-functionalized LNA monomers present themselves as interesting candidates for gene targeting applications in molecular biology and biotechnology.

SUPPLEMENTARY DATA

Supplementary Data are available at NAR Online: Supplementary Table 1 and Supplementary Data.

ACKNOWLEDGEMENTS

FUNDING

REFERENCES

1. Mukherjee,A. and Vasquez,K.M. (2011) Triplex technology in studies of DNA damage, DNA repair and mutagenesis. *Biochimie*, **93**, 1197–1208.
2. Ghosh,I., Stains,C.I., Ooi,A.T. and Segal,D.J. (2006) Direct detection of double-stranded DNA: molecular methods and applications for DNA diagnostics. *Mol. BioSyst.*, **2**, 551–560.
3. Dervan,P.B., Doss,R.M. and Marques,M.A. (2005) Programmable DNA binding oligomers for control of transcription. *Curr. Med. Chem. Anti-Cancer Agents*, **5**, 373–387.
4. Nielsen,P.E. (2010) Peptide nucleic acids (PNA) in chemical biology and drug discovery. *Chem. Biodiversity*, **7**, 786–804.
5. Rapireddy,S., Bahal,R. and Ly,D.H. (2011) Strand invasion of mixed-sequence, double-helical B-DNA by γ-peptide nucleic acids containing G-clamp nucleobases under physiological conditions. *Biochemistry*, **50**, 3913–3918.
6. Lohse,J., Dahl,O. and Nielsen,P.E. (1999) Double duplex invasion by peptide nucleic acid: a general principle for sequence-specific targeting of double-stranded DNA, *Proc. Natl Acad. Sci. USA*, **96**, 11804–11808.
7. Ishizuka,T., Yoshida,J., Yamamoto,Y., Sumaoka,J., Tedeschi,T., Corradini,R., Sforza,S. and Komiyama,M. (2008) Chiral introduction of positive charges to PNA for double-duplex invasion to versatile sequences. *Nucleic Acids Res.*, **36**, 1464–1471.
8. Beane,R., Gabillet,S., Montaillier,C., Arar,K. and Corey,D.R. (2008) Recognition of chromosomal DNA inside cells by locked nucleic acids. *Biochemistry*, **47**, 13147–13149.
9. Sau,S.P., Kumar,T.S. and Hrdlicka,P.J. (2010) Invader LNA: efficient targeting of short double stranded DNA. *Org. Biomol. Chem.*, **8**, 2028–2036.
10. Duca,M., Vekhoff,P., Oussedik,K., Halby,L. and Arimondo,P.B. (2008) The triple helix: 50 years later, the outcome. *Nucleic Acids Res.*, **36**, 5123–5138.
11. Puri,N., Majumdar,A., Cuenoud,B., Miller,P.S. and Seidman,M.M. (2004) Importance of clustered 2′-O-(2-aminoethyl) residues for the gene targeting activity of triple helix-forming oligonucleotides. *Biochemistry*, **43**, 1343–1351.
12. Mergny,J.-L. and Lacroix,L. (2003) Analysis of thermal melting curves. *Oligonucleotides*, **13**, 515–537.
13. Rusling,D.A., Broughton-Head,V.J., Tuck,A., Khairallah,H., Osborne,S.D., Brown,T. and Fox,K.R. (2008) Kinetic studies on the formation of DNA triplexes containing the nucleoside analogue 2′-O-(2-aminoethyl)-5-(3-amino-1-propynyl)uridine. *Org. Biomol. Chem.*, **6**, 122–129.
14. Rougee,M., Faucon,B., Mergny,J.-L., Barcelo,F., Giovannangeli,C., Garestier,T. and Hélène,C. (1992) Kinetics and thermodynamics of triple-helix formation: effects of ionic strength and mismatches. *Biochemistry*, **31**, 9269–9278.
15. Protozanova,E. and Macgregor,R.B. (1996) Kinetic footprinting of DNA triplex formation. *Anal. Biochem.*, **243**, 92–99.
16. Paes,H. and Fox,K.R. (1997) Kinetic studies on the formation of intermolecular triple helices. *Nucleic Acids Res.*, **25**, 3269–3274.
17. Bates,P.J., Dosanjh,H.S., Kumar,S., Jenkins,T.C., Laughton,C.A. and Neidle,S. (1995) Detection and kinetic studies of triplex formation by oligodeoxynucleotides using real-time biomolecular interaction analysis (BIA). *Nucleic Acids Res.*, **23**, 3627–3632.
18. Torigoe,H., Hari,Y., Sekiguchi,M., Obika,S. and Imanishi,T. (2001) 2′-O,4′-C-methylene bridged nucleic acid modification promotes pyrimidine motif triplex DNA formation at physiological pH: thermodynamic and kinetic studies. *J. Biol. Chem.*, **276**, 2354–2360.
19. Xodo,L.E. (1995) Kinetic analysis of triple-helix formation by pyrimidine oligodeoxynucleotides and duplex DNA. *Eur. J. Biochem.*, **228**, 918–926.
20. Yang,M., Ghosh,S.S. and Millar,D.P. (1994) Direct measurement of thermodynamic and kinetic parameters of DNA triple helix formation by fluorescence spectroscopy. *Biochemistry*, **33**, 15329–15337.
21. Tse,W.C. and Boger,D.L. (2004) A fluorescent intercalator displacement assay for establishing DNA binding selectivity and affinity. *Acc. Chem. Res.*, **37**, 61–69.
22. Lewis,M.A. and Long,E.C. (2006) Fluorescent intercalator displacement analyses of DNA binding by the peptide-derived natural products netropsin, actinomycin and bleomycin. *Bioorg. Med. Chem.*, **14**, 3481–3490.
23. Krishnamurthy,M., Schirle,N.T. and Beal,P.A. (2008) Screening helix-threading peptides for RNA binding using a thiazole orange displacement assay. *Bioorg. Med. Chem.*, **16**, 8914–8921.
24. Hauschild,K.E., Stover,J.S., Boger,D.L. and Ansari,A.Z. (2009) CSI-FID: high throughput label-free detection of DNA binding molecules. *Bioorg. Med. Chem. Lett.*, **19**, 3779–3782.
25. Yeung,B.K.S., Tse,W.C. and Boger,D.L. (2003) Determination of binding affinities of triplex forming oligonucleotides using a fluorescent intercalator displacement (FID) assay. *Bioorg. Med. Chem. Lett.*, **13**, 3801–3804.
26. Kaur,H., Babu,B.R. and Maiti,S. (2007) Perspectives on chemistry and therapeutic applications of Locked Nucleic Acid (LNA). *Chem. Rev.*, **107**, 4672–4697.
27. Koshkin,A.A., Singh,S.K., Nielsen,P., Rajwanshi,V.K., Kumar,R., Meldgaard,M., Olsen,C.E. and Wengel,J. (1998) LNA (Locked Nucleic Acids): synthesis of the adenine, cytosine, guanine, 5-methylcytosine, thymine and uracil bicyclonucleoside monomers, oligomerisation and unprecedented nucleic acid recognition. *Tetrahedron*, **54**, 3607–3630.
28. Obika,S., Hari,Y., Sugimoto,T., Sekiguchi,M. and Imanishi,T. (2000) Triplex-forming enhancement with high sequence selectivity by single 2′-O,4′-C-methylene bridged nucleic acid (2′,4′-BNA) modification. *Tetrahedron Lett.*, **41**, 8923–8927.
29. Sørensen,M.D., Kværnø,L., Bryld,T., Håkansson,A.E., Verbeure,B., Gaubert,G., Herdewijn,P. and Wengel,J. (2002) α-L-ribo-configured locked nucleic acid (α-L-LNA): synthesis and properties. *J. Am. Chem. Soc.*, **124**, 2164–2176.
30. Obika,S., Uneda,T., Sugimoto,T., Nanbu,D., Minami,T., Doi,T. and Imanishi,T. (2001) 2′-O,4′-C-methylene bridged nucleic acid (2′,4′-BNA). *Bioorg. Med. Chem.*, **9**, 1001–1011.
31. Sørensen,J.J., Nielsen,J.T. and Petersen,M. (2004) Solution structure of a dsDNA:LNA triplex. *Nucleic Acids Res.*, **32**, 6078–6085.

32. Sun,B.-W., Babu,B.R., Sørensen,M.D., Zakrzewska,K., Wengel,J. and Sun,J.-S. (2004) Sequence and pH effects of LNA-containing triple helix-forming oligonucleotides: physical chemistry, biochemistry and modeling studies. *Biochemistry*, **43**, 4160–4169.

33. Brunet,E., Alberti,P., Perrouault,L., Babu,R., Wengel,J. and Giovannangeli,C. (2005) Exploring cellular activity of locked nucleic acid-modified triplex-forming oligonucleotides and defining its molecular basis. *J. Biol. Chem.*, **280**, 20076–20085.

34. Kumar,N., Nielsen,K.E., Maiti,S. and Petersen,M. (2006) Triplex formation with alpha-L-LNA (alpha-L-ribo-configured locked nucleic acid). *J. Am. Chem. Soc.*, **128**, 14–15.

35. Torigoe,H., Rahman,S.M.A., Takuma,H., Sato,N., Imanishi,T., Obika,S. and Sasaki,K. (2011) 2′-O,4′-C-aminomethylene-bridged nucleic acid modification with enhancement of nuclease resistance promotes pyrimidine motif triplex nucleic acid formation at physiological pH. *Chem. Eur. J.*, **17**, 2742–2751.

36. Rahman,S.M.A., Seki,S., Obika,S., Haitani,S., Miyashita,K. and Imanishi,T. (2007) Highly stable pyrimidine-motif triplex formation at physiological pH values by a bridged nucleic acid analogue. *Angew. Chem. Int. Ed.*, **46**, 4306–4309.

37. Højland,T., Kumar,S., Babu,B.R., Umemoto,T., Albaek,N., Sharma,P.K., Nielsen,P. and Wengel,J. (2007) LNA (locked nucleic acid) and analogs as triplex-forming oligonucleotides. *Org. Biomol. Chem.*, **5**, 2375–2379.

38. Koizumi,M., Morita,K., Daigo,M., Tsutsumi,S., Abe,K., Obika,S. and Imanishi,T. (2003) Triplex formation with 2′-O,4′-C-ethylene-bridged nucleic acids (ENA) having C3′-endo conformation at physiological pH. *Nucleic Acids Res.*, **31**, 3267–3273.

39. Torigoe,H., Nakagawa,O., Imanishi,T., Obika,S. and Sasaki,K. (2012) Chemical modification of triplex-forming oligonucleotide to promote pyrimidine motif triplex formation at physiological pH. *Biochimie*, **94**, 1032–1040.

40. Kumar,S., Hansen,M.H., Albaek,N., Steffansen,S.I., Petersen,M. and Nielsen,P. (2009) Synthesis of functionalized carbocyclic locked nucleic acid analogues by ring-closing diene and enyne metathesis and their influence on nucleic acid stability and structure. *J. Org. Chem.*, **74**, 6756–6769.

41. Bijapur,J., Keppler,M.D., Bergqvist,S., Brown,T. and Fox,K.R. (1999) 5-(1-propargylamino)-2′-deoxyuridine (UP): a novel thymidine analogue for generating DNA triplexes with increased stability. *Nucleic Acids Res.*, **27**, 1802–1809.

42. Brazier,J.A., Shibata,T., Townsley,J., Taylor,B.F., Frary,E., Williams,N.H. and Williams,D.M. (2005) Amino-functionalized DNA: the properties of C5-amino-alkyl substituted 2′-deoxyuridines and their application in DNA triplex formation. *Nucleic Acids Res.*, **33**, 1362–1371.

43. Lacroix,L., Lacoste,J., Reddoch,J.F., Mergny,J.-L., Levy,D.D., Seidman,M.M., Matteucci,M.D. and Glazer,P.M. (1999) Triplex formation by oligonucleotides containing 5-(1-propynyl)-2′-deoxyuridine: decreased magnesium dependence and improved intracellular gene targeting. *Biochemistry*, **38**, 1893–1901.

44. Phipps,A.K., Tarköy,M., Schultze,P. and Feigon,J. (1998) Solution structure of an intramolecular DNA triplex containing 5-(1-propynyl)-2′-deoxyuridine residues in the third strand. *Biochemistry*, **37**, 5820–5830.

45. Li,H., Miller,P.S. and Seidman,M.M. (2008) Selectivity and affinity of DNA triplex forming oligonucleotides containing the nucleoside analogues 2′-O-methyl-5-(3-amino-1-propynyl)uridine and 2′-O-methyl-5-propynyluridine. *Org. Biomol. Chem.*, **6**, 4212–4217.

46. Lou,C., Xiao,Q., Brennan,L., Light,M.E., Vergara-Irigaray,N., Atkinson,E.M., Holden-Dye,L.M., Fox,K.R. and Brown,T. (2010) Synthesis and properties of triplex-forming oligonucleotides containing 2′-O-(2-methoxyethyl)-5-(3-aminoprop-1-ynyl)-uridine. *Bioorg. Med. Chem.*, **18**, 6389–6397.

47. Sollogoub,M., Darby,R.A.J., Cuenoud,B., Brown,T., Fox,K.R., Coman,D. and Russu,I.M. (2002) Stable DNA triple helix formation using oligonucleotides containing 2′-aminoethoxy-5-propargylamino-U. *Biochemistry*, **41**, 7224–7231.

48. Østergaard,M.E., Kumar,P., Baral,B., Raible,D.J., Kumar,T.S., Anderson,B.A., Guenther,D.C., Deobald,L., Paszczynski,A.J. and Sharma,P.K. (2009) C5-functionalized LNA: unparalleled hybridization properties and enzymatic stability. *ChemBioChem*, **10**, 2740–2743.

49. Sau,S.P., Kumar,P., Anderson,B.A., Østergaard,M.E., Deobald,L., Paszczynski,A., Sharma,P.K. and Hrdlicka,P.J. (2009) Optimized DNA-targeting using triplex forming C5-alkynyl functionalized LNA. *Chem. Commun.*, 6756–6758.

50. Mergny,J.-L., Collier,D., Rougee,M., Montenay-Garestier,T. and Hélène,C. (1991) Intercalation of ethidium bromide into oligonucleotide. *Nucleic Acids Res.*, **19**, 1521–1526.

51. Maher,L.J., Dervan,P.B. and Wold,B. (1990) Kinetic analysis of oligodeoxyribonucleotide-directed triple-helix formation on DNA. *Biochemistry*, **29**, 8820–8826.

52. Sugimoto,N., Wu,P., Hara,H. and Kawamoto,Y. (2001) pH and cation effects on the properties of parallel pyrimidine motif DNA triplexes. *Biochemistry*, **40**, 9396–9405.

53. Lee,J.S., Woodsworth,M.L., Latimer,L.J.P. and Morgan,A.R. (1984) Poly(pyrimidine) poly(purine) synthetic DNAs containing 5-methylcytosine form stable triplexes at neutral pH. *Nucleic Acids Res.*, **12**, 6603–6614.

54. Scaria,P.V. and Shafer,R.H. (1991) Binding of ethidium bromide to a DNA triple helix. Evidence for intercalation. *J. Biol. Chem.*, **266**, 5417–5423.